Supporting Information

Canfield et al. 10.1073/pnas.1315570110

SI Text

Sample Collection, Trace Metal Analysis, and Iron Speciation

Samples were collected from both outcrop and drill core material, with similar results in overlapping strata. Iron speciation analyses followed ref. 1 whereas sulfur (relative to Cañon Diablo troilite) and carbon (relative to PDB) isotope analyses were performed by isotope ratio mass spectrometry (Thermo Delta plus) following combustion in an elemental analyzer. Trace metals were determined after first powdering rock samples (300 mg) and then fusion along with 900 mg of ultra-pure $LiBO_2$ at 980 °C in an automatic tunnel oven. Samples were passed through the oven on a rail over a period of about 60 min at a constant speed, ensuring that all of the samples encountered the same thermal gradient. After cooling to room temperature, the fusion glass was dissolved in an HNO_3 (1 mol/L)-H_2O_2 (0.5%)-glycerol (10%, vol/vol) mixture to a dilution factor of 333 relative to the amount of sample fused. Trace metals were measured by inductively coupled plasma mass spectrometry (ICP-MS) (Thermo ×7) using a one point "linear through zero" calibration whereas major elements were determined by inductively coupled plasma-optical emission spectrometry (ICP OES) (Thermo Icap 6500). Organic carbon concentrations were determined after acid treatment to remove carbonate using a Leco SC144 DR whereas sulfur contents were determined by either weighing Ag_2S precipitates after Cr distillation of the samples to liberate reduced sulfur (2), or directly with the Leco SC144 DR. Molybdenum isotopes were determined by multi-collector plasma-optical emission spectrometry (MC-ICP-MS), with a full description in *Mo-Isotope Analyses*. Relative sea level trends were determined by lithofacies study on the whole Francevillian group based on direct observations of outcrops and cores.

Mo-Isotope Analyses

Due to the high content of organic matter, all samples were ashed in quartz beakers at 600 °C for at least 24 h. All later chemical procedures were undertaken in clean laboratories, using distilled acid (HNO_3; HCl) or trace metal grade HF. About 200 mg of ashed sample was dissolved in concentrated HNO_3 (7 mL) + HF (1.5 mL) and evaporated on a hot plate at 60 °C. Dry residues were further dissolved with concentrated HNO_3 + HCl, taken to dryness, and finally redissolved with 20 mL of 7N HCl. Depending on the Mo concentration, a portion of each sample solution was doped with Mo double spike to keep a constant spike/sample ratio, and the samples were then subject to chromatographic separation as described in refs. 3 and 4. Briefly, Mo purification was done in a two-stage column procedure: in the first stage, an anion resin separated Mo (Biorad AG-MP1) and most of the Fe from the matrix, and in a second stage, a cation resin separated Mo from the remaining Fe (Biorad AG-50 × 8). Mo isotope composition measurements were done using a Thermo Neptune MC-ICP-MS instrument at the Pole Spectrometrie Ocean, Brest at IFREMER (France).

We used ^{97}Mo-^{100}Mo double-spike solution prepared gravimetrically from Oak Ridge Laboratory metal powders. Optimization of the double-spike isotope composition relative to the SPEX standard gave $^{95}Mo/^{98}Mo$, $^{97}Mo/^{98}Mo$, and $^{100}Mo/^{98}Mo$ isotopic ratios of 0.278, 16.663, and 15.704, respectively. Data reduction was done according to ref. 5 where iterations were repeating while the difference in the $\delta^{98}Mo$ value between two consecutive iterations was smaller than 0.001‰. The typical number of iterations was ≤4. Molybdenum concentrations varied from 100 to 500 parts per billion (ppb), depending on the Mo content of the sample powders. Within each session, standards and samples were measured at a constant concentration. The external precision of the measurement was $2\sigma = \pm 0.04‰$ whereas the typical SE of a single measurement was $2\sigma = 0.05‰$. Molybdenum concentrations were derived from the spike/sample ratio determined as part of the double-spike data reduction scheme. The MC-ICP-MS machine was operated at low resolution with an ESI Apex Q introduction system measuring all Mo isotope masses together with ^{91}Zr and ^{99}Ru to monitor isobaric interferences.

During each session of Mo-isotope measurements, we performed frequent measurements of our in-house laboratory Mo standard (Mo SPEX lot 11–177Mo), measurements of the NIST-3137 standard, and the Johnson Matthey Specpure Mo plasma standards (Lot no. 802309E; RochMo2) used in previous studies (3). We also preformed frequent measurements of geo-reference materials including SDO-1, Nod A-1, and Nod P-1.

Molybdenum isotopic compositions are all reported here using the δ notation (in terms of $^{98}Mo/^{95}Mo$ ratios) calculated relative to our in-laboratory Mo SPEX standard (lot 11–177Mo). A calibration of the SPEX standard relative to NIST-3137 (lot 891307) and Rochester (lot 802309E) standards (supplied by the laboratory of A. D. Anbar, Arizona State University) gave:

$$\delta^{98/95}Mo_{SPEX} = \delta^{98/95}Mo_{NIST3137} - 0.35 \pm 0.06‰$$
$$\delta^{98/95}Mo_{SPEX} = \delta^{98/95}Mo_{Mo\text{-}Roch} - 0.05 \pm 0.03‰.$$

We choose to report our results relative to the SPEX standard because, within error, it is identical to the Rochester standard, which is the most common standard in recent Mo-isotope literature.

Shungite Depositional Environment

The most comprehensive description of shungite chemistry comes from the study of ref. 6. The distribution of C/S ratios from these sediments falls within the range of nonmarine fresh-water sediments, leading the authors to conclude that "the sediments deposited in swampy, brackish water lagoon under noneuxinic condition." However, the shungites are not well-suited to environmental interpretations based on C/S ratios because the shungites are extremely rich in organic carbon, approaching 100% in some cases, and very poor in Fe (Table S1). Thus, there is insufficient Fe to capture the sulfide produced by sulfate reduction, making the C/S ratio of little use in environmental interpretations (Table S1). The shungites, however, are rich in Mo and V, to the same level as the euxinic Francevillian sediments and thus are completely consistent with deposition in a euxinic environment. The shungites also have high ratios of pyrite Fe (FePy)/total Fe (FeT). In many cases, it appears that all or nearly all of the Fe is completely pyritized. In other cases, some of the Fe is clearly not pyritized, but anoxic sediments deposited in euxinic environments can have FePy/FeT ratios between about 0.3 and 1.0 [the low end is with highly reactive Fe (FeHR)/FeT of 0.4 and FePy/FeHR of 0.7 whereas, in the upper end, both of these ratios are 1]. A direct comparison with modern depositional environment would be possible if highly reactive Fe contents were available, but they unfortunately are not.

---

1. Poulton SW, Canfield DE (2005) Development of a sequential extraction procedure for iron: Implications for iron partitioning in continentally-derived particulates. *Chem Geol* 214:209–221.

2. Canfield DE, Raiswell R, Westrich JT, Reaves CM, Berner RA (1986) The use of chromium reduction in the analysis of reduced inorganic sulfur in sediments and shales. *Chem Geol* 54:149–155.

3. Barling J, Arnold GL, Anbar AD (2001) Natural mass-dependent variations in the isotopic composition of molybdenum. *Earth Planet Sci Lett* 193(3-4):447–457.
4. Wille M, et al. (2007) Evidence for a gradual rise of oxygen between 2.6 and 2.5 Ga from Mo isotopes and Re-PGE signatures in shales. *Geochim Cosmochim Acta* 71(10): 2417–2435.
5. Siebert C, Nagler TF, Kramers JD (2001) Determination of molybdenum isotope fractionation by double-spike multicollector inductively coupled plasma mass spectrometry. *Geochem Geophys Geosyst* 2:2000GC000124.
6. Melezhik VA, Fallick AE, Filippov MM, Larsen O (1999) Karelian shungite-an indication of 2.0-Ga-old metamorphosed oil-slae and generation of petroleum: Geology, lithology and geochemistry. *Earth Sci Rev* 47:1–40.

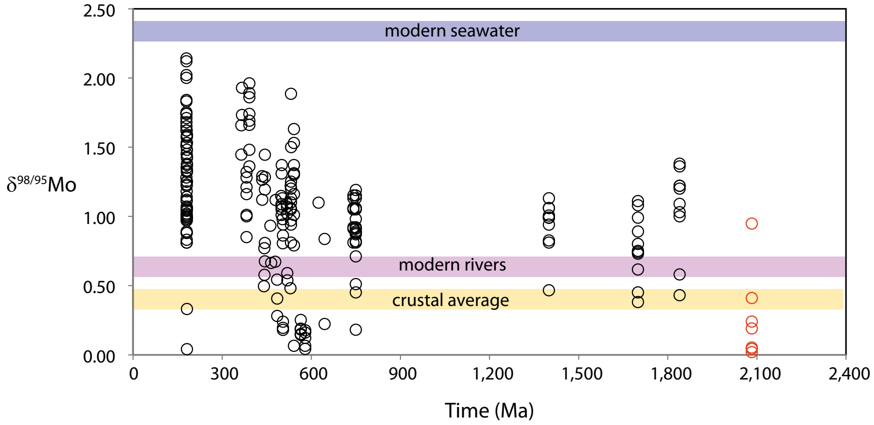

Fig. S1. The isotopic composition of Mo ($\delta^{98/95}$Mo) since the GOE. Data from Gabon are shown in red. Other data are from the compilation presented in ref. 1; original references can be found there.

1. Raiswell R, Canfield DE (2012) The iron biogeochemical cycle past and present. *Geochem Perspect* 1(1):1–220.

Table S1. Data for *ca*. 2.1 Ga Fennoscandian shungites (from ref. 6)

Sample	TOC	S, wt%	Fe, wt%	FePy/FeT	Mo, ppm	Mo/TOC	V, ppm
1	2.0	B.D.	0.10		41	20.5	59
2	37.7	0.1	0.17	0.52	7	0.18	117
3	35.5	B.D.	0.11		10	0.28	127
4	31.4	0.4	1.07	0.32	12	0.38	154
5	N.D.	0.5	0.61	0.72	49		416
6	N.D.	2.2	1.41	1.37	38		483
7	1.0	B.D.	0.10		7	7.0	46
8	1.4	B.D.	0.08		8	5.71	78
9	64.1	5.0	7.66	0.57	237	3.70	1,304
10	56.7	3.8	6.72	0.49	258	4.55	1,667
11	98.4	0.2	N.D		168	1.71	940
12	90.0	0.6	0.13	4.16	B.D.		54
13	0.9	B.D.	9.67		B.D.		227
14	25.2	B.D.	0.87		40	1.59	589
15	45.5	B.D.	0.18		86	1.89	593

B.D., below detection; Ga, billion years ago; N.D., not determined; ppm, parts per million; TOC, total organic carbon.

Table S2. Data from Francevillian samples of the current study

Formations	Mo,ppm	U, ppm	Fe, wt%	Al, wt%	Mn, wt%	V, ppm	FeHR/FeT	FePy/FeHR	S, wt%	$\delta^{34}S$	TOC, wt%	δ^{13}Corg	$\delta^{98/95}$Mo
	22.18	6.01	0.00	6.97	0.01	259.60					9.40	−46.00	0.02
	31.91	6.73	5.30	5.65	0.03	270.00	0.76	0.90	4.03	0.64	10.90	−45.98	0.05
	39.70	5.43	6.25	6.17	0.05	283.30			5.52				
	34.40	4.68	5.71	6.56	0.08	247.90	0.75	0.90	4.35	6.07	9.32	−45.68	0.04
	40.20	5.38	4.29	6.54	0.09	256.00	0.49	0.79	3.26		9.30	−45.70	
FD	28.04	5.74	5.77	6.10	0.22	230.60	0.69	0.87	4.17	23.99	8.60	−45.20	0.41
	43.20	6.63	6.41	5.10	0.02	281.60	0.90	0.87	6.02		10.64	−45.22	
	41.30	6.73	4.54	5.29	0.06	393.20			3.71				
	31.69	6.15	4.48	5.34	0.01	275.90	0.65	0.80	3.42	3.69	9.10	−46.10	0.19
	30.41	4.52	4.94	5.66	0.05	247.40	0.81	0.61	3.46	5.43	9.80	−46.20	0.24
	5.28	5.48	5.92	5.39	0.15	105.60	0.81	0.69	3.71		8.60	−48.00	0.95
											9.90	−46.20	
	2.65	4.40	4.01	4.58	0.13	162.60	0.44	0.53	1.25	−1.84	5.90	−46.30	
			0.00	0.00							10.57	−40.40	
	< L.D	0.99	1.93	1.91	1.14	10.00	0.46	0.61	0.90	−0.21	3.10	−43.30	
	27.00	6.23	2.39	2.90	0.01	571.90	0.93	0.89	2.53	−1.82	10.87	−31.98	
							0.93	0.85		−3.77	0.82	−41.17	
	64.80	7.83	5.35	3.59	0.04	652.20	0.83	0.72	5.84		7.80	−38.80	
	3.59	1.82	1.60	0.29	0.01	7.10			1.71				
FC	1.47	1.52	0.28	7.06	0.00	56.12	0.18	0.25	0.10		8.22	−35.12	
	1.42	1.53	0.28	7.47	0.00	60.20	0.27	0.27	0.09		6.51	−35.09	
	1.31	1.25	1.48	0.79	0.03	30.10			1.38				
											2.00	−37.10	
	10.65	3.47	2.37	2.29	0.01	200.30			2.51				
	0.33	1.22	0.88	8.46	0.02	46.55			0.13		—	—	
	0.47	1.73	1.34	10.74	0.02	65.63	0.17	0.51	0.16	4.95	5.80	−32.60	
											2.59	−32.46	
	1.67	1.88	1.85	9.09	0.04	65.32	0.65	0.65	1.08	−9.30	8.40	−32.95	
	0.51	1.62	2.28	10.50	0.15	63.87	0.26	0.29	0.07	−17.10	7.30	−32.50	
	0.51	1.58	2.81	10.14	0.14	66.66					5.00	−32.40	
	0.50	1.54	3.33	9.77	0.13	69.45	0.08	0.27	0.05	−2.42	3.80	−33.46	
											2.65	−33.55	
FB2b							0.14	0.32		−7.70			
							0.33	0.04		25.00			
							0.27	0.14		−11.87			
							0.37	0.24		−8.88			
	0.76	1.21	2.41	9.87	0.05	52.97	0.35	0.13		−13.59	2.33	−35.10	
	0.76	1.08	4.54	6.38	0.57	32.39	0.14	0.37		−10.60	2.30	−34.60	
	0.72	1.02	6.20	6.37	0.08	29.13					0.12	−32.70	
	2.92	1.00	0.29	8.28	0.00	92.65					0.39	−30.15	
							0.90	0.62	1.16	10.14	6.10	−34.11	
	0.58	1.16	2.80	6.63	0.06	49.35	0.78	0.61	2.96	13.98	6.70	−35.00	0.30
							1.10	0.78	1.03	11.07	3.93	−35.11	
	1.15	0.95	0.94	4.37	1.46	46.10	1.13	0.82	0.96	10.88	4.80	−33.80	
	1.82	0.80	2.09	5.81	5.41	80.00						−34.60	
							1.19	0.72	1.45	14.65	4.35	−34.16	
	7.05	0.19	0.50	1.35	13.89	20.45	0.91	0.55	0.55	9.30	1.30	−33.60	−0.74
			2.12	3.48	11.75		0.80	0.28	0.40	9.58	3.32	−33.77	
	2.75	1.07	2.49	5.29	13.65	50.81			1.63		11.50	−34.49	
			1.87	3.70	13.19		0.93	0.33	0.37	8.43	6.68	−33.58	
			1.76	3.64	9.23						7.60	−33.70	
			2.18	7.57	6.13		0.84	0.58	1.47	9.06	4.87	−34.07	
	3.57	1.11	2.01	6.46	0.09	47.24			1.89				
	24.77	0.78	1.88	3.26	19.63	77.59			1.97		6.70	−34.02	
			1.88	4.55	0.83		1.17	0.65	1.19	11.23	9.70	−34.00	
	5.57	0.62	1.52	3.14	16.14	48.54			1.61		6.00	−33.86	−0.59
			1.23	2.43	14.16						5.40	−33.30	
			1.38	2.23	14.60		1.17	0.64	1.11	10.71	3.05	−32.69	
			1.38	2.12	15.67		1.17	0.64	1.11	11.57	1.74	−32.39	
	3.48	0.46	1.56	2.18	21.15	30.65	0.90	0.50	1.57		3.70	−33.12	

Table S2. Cont.

Formations	Mo,ppm	U, ppm	Fe, wt%	Al, wt%	Mn, wt%	V, ppm	FeHR/FeT	FePy/FeHR	S, wt%	δ^{34}S	TOC, wt%	δ^{13}Corg	$\delta^{98/95}$Mo
	7.09	1.25	2.47	3.85	9.78	58.51	0.98	0.55	2.66	11.26	2.80	−33.20	−0.16
	1.33	0.42	1.79	2.31	16.84	38.50	0.92	0.73	1.76	8.32	3.60	−32.40	
							0.78	0.25	1.20	−0.64	1.30	−32.31	
FB1c	3.03	1.00	3.12	3.60	16.19	39.57	0.66	0.48	3.62	5.80	3.60	−31.30	
	0.63	0.35	6.75	1.38	17.16	16.76	0.64	0.34		−2.09	0.12	−31.36	−0.25
							0.76	0.34	1.22	−7.27	0.55	−30.89	
	1.00	1.49	1.82	5.41	0.17	60.74	1.04	0.90	1.86	−6.88	8.30	−30.20	
	2.31	2.61	2.05	6.80	0.06	82.52	1.08	0.85	1.99	−7.91	8.40	−30.10	
	2.57		35.91	0.09	0.49	2.05			0.05				
	0.59	2.03	1.78	6.01	0.09	42.08	0.21	0.79	1.25	−6.93	8.90	−28.80	
							0.78	0.79		−7.37	1.65	−29.48	
							0.69	0.56		−14.74	0.49	−29.99	
	3.07	0.95	3.07	4.20	0.10	17.42	1.02	0.90	2.90	−11.28	5.50	−27.80	
							0.37	0.02		−3.47	0.32		
							0.54	0.01	0.01	−16.97	0.20	−28.71	
											1.50	−27.42	
	1.67	1.39	3.80	5.23	0.05	95.80	0.52	0.64	1.30	−29.89	1.30	−27.06	
							0.67	0.23	0.30	−26.17	0.30		
	0.64	1.01	1.79	6.60	0.01	27.57					3.10	−26.78	
											2.10	−27.17	
											1.70	−27.65	
											0.90	−26.51	
							0.71	0.39	0.48	−31.97	2.00	−27.47	
							0.37	0.02	0.48	−3.47	0.40	−26.91	
							0.17	0.10			1.60	−26.90	
							0.31	0.10		−18.41	0.20	−26.52	
											0.30	−26.49	
			3.11	7.41			0.17	0.10	0.03	−8.94	0.33	−28.19	
							0.11	0.08	0.02	−19.65	0.26	−26.61	
			3.11	10.06			0.16	0.39	0.10	−24.96	2.82	−26.37	
							0.28	0.29		−30.25	6.82	−24.54	
							0.37	0.36		−29.20	2.33	−24.37	
	0.73	2.03	5.43	10.34	0.07	62.89	0.12	0.12	0.08		7.20	−24.50	1.31
							0.35	0.44	0.39	−32.41	14.29	−21.91	
	1.71	116.60	1.07	9.52	0.00	108.90			0.19		7.10	−22.90	
							0.36	0.34		−4.05			
							0.52	0.69		−25.07			
							0.17	0.36		−10.11			
	0.49	1.60	3.09	6.35	0.27	39.22					3.72		
	0.38	0.20	1.08	0.83	0.18	5.08					3.60	−23.92	
	< L.D	1.74	2.43	9.41	0.31	65.03	0.07	0.06	0.03	−9.71	3.80	−24.16	
							0.12	0.20	0.05	−22.84			
							0.31	0.20	0.12	−24.15			
	0.42	3.26	2.17	8.85	0.35	69.40	0.43	0.42	0.27	−31.74	7.80	−24.11	
							0.43	0.48	0.58	−20.73	0.17	−24.46	
							0.42	0.47	0.45	−26.95	0.19	−26.08	
							0.46	0.48	0.56	−20.06	0.11	−25.55	
							0.36	0.40	0.40	−24.96		−25.10	
	0.54	3.36	3.12	7.84	0.41	56.20	0.36	0.28	0.28	−24.60	6.00	−23.90	−1.10
	1.55	0.45	8.60	2.26	0.85	14.00	0.57	0.01	0.39	−10.81	2.10	−23.70	−0.30
FB1b	0.75	2.58	2.47	8.15	0.20	46.02	0.40	0.37	0.45	−23.47	6.50	−23.42	−0.09
							0.36	0.36	0.35	−22.74	1.94	−25.06	
							0.37	0.58	0.54	−22.59	4.88	−24.32	
							0.30	0.49	0.51	−19.77			
							0.30	0.53	0.38	−20.71			
	0.33	2.31	1.32	12.01	0.02	113.30	0.22	0.17	0.11	−10.87	7.60	−24.44	
							0.13	0.04	0.01	−1.62			
	2.37	0.85	22.99	2.17	0.60	40.78	0.48	0.20	21.00	−25.44	4.20	−24.50	
	0.42	2.46	6.41	7.81	0.02	43.62	0.17	0.11	0.06	−23.11	0.70	−23.68	
							0.08	0.08	0.01	−25.99			
							0.09	0.15	0.03	−27.28			

Table S2. Cont.

Formations	Mo,ppm	U, ppm	Fe, wt%	Al, wt%	Mn, wt%	V, ppm	FeHR/FeT	FePy/FeHR	S, wt%	δ^{34}S	TOC, wt%	δ^{13}Corg	$\delta^{98/95}$Mo
							0.06	0.15	0.02	−24.71			
							0.07	0.08	0.06	−23.39			
	< L.D	1.32	1.81	11.02	0.00	59.51	0.14	0.10	0.03		3.30	−24.65	
							0.17	0.10	0.04	−18.09			
							0.09	0.09	0.02	−17.86			
							0.24	0.46	0.43	−21.44			
							0.17	0.37	0.15	−21.73			
									0.02	−20.58	3.80	−23.95	
							0.09	0.04	0.02	−21.55			
							0.09	0.12	0.05	−19.04			
							0.16	0.08		−22.11			
	0.44	1.52	2.50	10.74	0.02	56.01	0.20	0.18	0.07	−22.94	3.30	−30.01	
							0.16	0.34	0.13	−23.61			
											4.10		
							0.10	0.14	0.04	−7.29			
							0.06	0.04	0.01	−23.32			
	1.09	2.00	2.82	12.72	0.02	71.57	0.33	0.10	0.01		0.60		
	3.91	2.43	4.43	10.36	0.01	83.90	0.66	0.74	3.62		8.50	−26.40	1.03
	0.54		2.19	12.03	0.00	71.32	0.03	0.06	0.01	22.11			
							0.03	0.06	0.00	−5.91			
							0.21	0.07	0.00	−25.65			
	0.58	1.29	2.87	13.17	0.01	33.39			0.01		—		
FB1a	0.32	1.38	3.34	11.29	0.01	50.59			0.01		—		
	0.32	2.08	4.31	15.62	0.02	53.85	0.15	0.56	0.00	−3.08	—		

—, below detection.